CHAPTER 3

Experimental Procedure

This chapter describes the development of induced-strain measurement system based on Michelson interferometer, which was used to observe induced-strain of ferroic materials caused by electric and magnetic field. This includes the setup of modified Michelson interferometer and the sample holder (and its environ) to measure electrostrictive properties at different aging conditions, frequencies and temperatures as well as magnetostrictive properties. First, a circular fringe pattern of Michelson interferometer had to be set up with designed sample holder for applied electric field to measure the displacement from interference intensity, and the real time results were detected by the digital oscilloscope which had interfaces to the computer for data recording and analysis. Second, the electric field at various frequencies was applied to ferroic samples to observe the frequency dependence of induced-strain behavior of ferroic samples. Third, the heat load sample holder was designed and set up for the induced-strain measurement to observe the temperature dependence of ferroic materials and phase transition behavior. Finally, the solenoid coil was designed to apply the magnetic field at the time of induced-strain measurement to observe magnetic field effect to induced-strain of ferroic samples.

3.1 Modified Michelson interferometer for induced-strain measurement system

Michelson interferometer technique has been well known because it is used in many applications such as small displacement measurement and surface analysis due to its high resolution, simple operation with no contact required and low cost. In this setup, Michelson interferometer utilized a polarized beam from a Helium-Neon laser source (MELLES GRIOT), with the uniphase wavelength (λ) of 632.8nm. The laser beam from laser source was split into two beams at the beam splitter and after that the beams reflected at the mirrors M_1 and M_2 (the surface coated mirror) then turned back to interfere on the screen as a circular fringe pattern, where the photodiode detector (PIN photodiode; p-type, intrinsic, n-type photodiode) was positioned at the center. To convert the interference intensity to the electrical signals as a voltage, a reverse bias circuit was used to detect signals from interference. The electrical signal was subjected to lower pass filtered process to eliminate electrical noise higher than 30 Hz and amplified the signal to 2-gain of the signal size by the low-noise preamplifier (Stanford Research system model SR 560). The amplified interference signal was detected by 14 bits digital oscilloscope (PicoScope) at the same time with the signal from Sawyer-Tower circuit which related to electrical polarization of ferroic samples, and high voltage 1/1000 reduced ratio signal which was applied to the ferroic samples. The high voltage signal for ferroic samples was generated from a 15 MHz signal generator (Rigol DG1012) which was connected to computer drawing and controling signal using Rigol Ultrawave program and was amplified by high voltage amplifier/controller supply (Trek 610D). All setups of modified Michelson interferometer, Sawyer-Tower circuit and sample holder were connected to the computer and fixed on the vibration freed optical table to eliminate the vibration noise as shown in Figure 3.1.

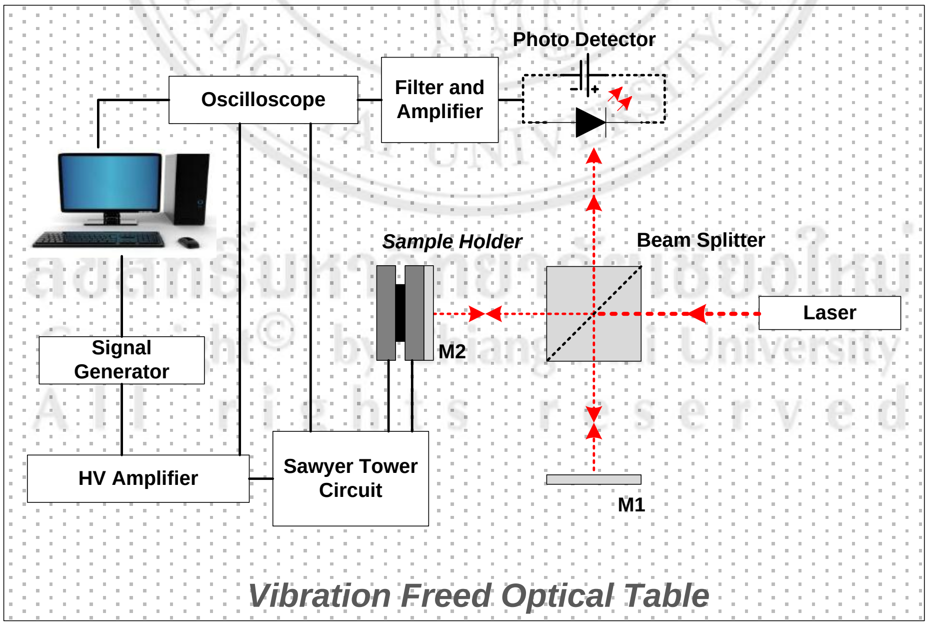

Figure 3.1 Schematic diagram of Modified Michelson interferometer for induced-strain measurement system

The sample holder was designed to fit the samples and to have a good contact by a spring load to keep the holder surface in contact with (close to) sample surface. The friction caused by the displacement resulting from electric field was remedied by placing the moving side of the sample holder on two parallel bearings. The high strength voltage amplifier was connected to the two sides of sample surface by passing through sample holder in the middle, where one side of sample holder was glued with the surface coated mirror (M_2) to reflect the laser beam from displaced samples as shown in Figure 3.2.

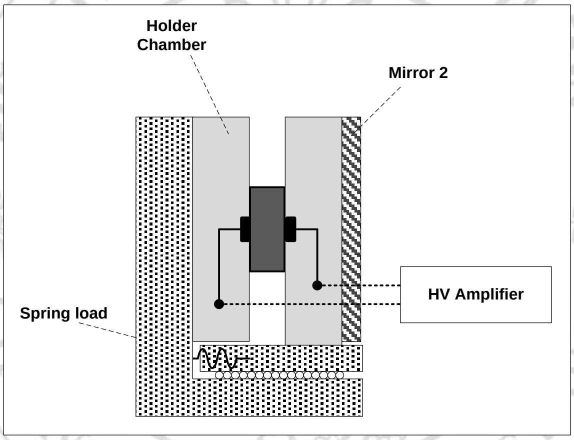

Figure 3.2 The sample holder

3.2 Investigation of electrostrictive properties using modified Michelson interferometer

3.2.1 Frequency dependence in induced-strain measurement for PMN-PZT

To observe frequency dependence of electric field induced-strain and polarization, the experimental setup is shown in Figure 3.1. The electric field induced-strain and polarization were measured for $0.7Pb(Mg_{1/3}Nb_{2/3})O_3–0.3Pb(Zr_{0.52}Ti_{0.48})O_3$ (1-x)PMN-xPZT relaxor ferroelectric ceramics where x = 0, 0.1, 0.3, 0.5 and 0.7 were prepared by solid state oxide mixing and consolidating by sintering method to investigate the effect of frequency to induced-strain and polarization behaviour. The frequencies used for the measurement were 1, 0.5, 0.2, 0.1, 0.05, 0.02 and 0.01 Hz. In the measurement, the sample surface of both sides was silver coated and placed in sample holder (Fig. 3.2). The sample was subjected to a bipolar high extension voltage at various frequencies; the high voltage was generated at signals generator (Rigol DG1012) and amplified by high voltage amplifier/controller supply (Trek 610D). The electrical signal from displacement interference intensity was filtered and amplified before detected together with Sawyer-Tower circuit signal and 1/1000 reduce ratio of high voltage signal by 14 bits digital oscilloscope (PicoScope), which had interface to record data at the computer where electric field induced-strain-polarization (s-P-E) and induced-strain as a function of polarization (s-P) were calculated, plotted and ferroelectric behavior as a function of frequency was analyzed.

3.2.2 Aging behavior in induced-strain measurement for 9/70/30 and 9/65/35 PLZT

The reliability in piezoelectric/electrostriction is the important result to ferroelectric actuator applications, which ferroelectric properties are changed after the first time of fabrication as a function of time. To observe time dependence of electric field induced strain and polarization, the experimental setup is shown in Figure 3.1. The electric field induced-strain and polarization at frequency of applied electric field of 0.2 Hz were measured for ferroelectric lead lanthanum zirconate tianate, $Pb_{0.91}La_{0.09}(Zr_{0.70}Ti_{0.30})_{0.9775}O_3$ PLZT (9/70/30) and $Pb_{0.91}La_{0.09}(Zr_{0.65}Ti_{0.35})_{0.9775}O_3$ PLZT (9/65/35) ceramics to investigate the effect of aging to induced-strain and polarization behavior. PLZT (9/70/30) and PLZT (9/65/35) ceramics powders were prepared by solid state oxide mixing following by calcination. The samples were made of powders by pressing into pellets then sintered at 1200, 1225, 1250 and 1275^{o}C for 2 hours. The samples were monitored the change regularly on day 1, 6, 11, 19 and 31 compared to the sample anneal at 600^{o}C for 1 hour to observe aging behaviour at room temperature. In the measurement, the silver coated sample surface process of PLZT was carried out for both sides before the electric field induced-strain measurement (Fig. 3.1) and the sample was placed in the sample holder (Fig. 3.2). The sample was subjected to a bipolar high extension voltage, where electrical signals from displacement interference intensity, Sawyer-Tower circuit and reduce ratio of high voltage were detected by digital oscilloscope, which had interface to record data at the computer where electric field induced-strain (s-E), polarization (P-E) and induced-strain as a function of polarization (s-P) were calculated, plotted and ferroelectric behavior of materials was analyzed.

3.2.3 Heat loading in induced-strain measurement system for PMN-PZT, PMN-PT and PLZT ceramics

In order to investigate the temperature dependence of ferroelectric materials in relation to the phase transition, the heat loaded sample holder is required. The operation was in the range from room temperature to 70°C and the temperature of the sample could be controlled and displayed with high accuracy (±0.5°C). The Michelson interferometer modified with heat load sample holder at the mirror M_2 is shown in Figure 3.3. The ceramic heater was selected for this propose and it was inserted inside the sample holder at the center where ceramics heater surface was attached to the sample surface to evenly distribute the heat to two sides of sample surface. The temperature of sample was a function of the electrical current (past through ceramic heater) applied from the programmable dc power supply (Rigol DP 1116A), and the temperature was detected by the integral circuit temperature detector (AD592 CN; the temperature range 0-120°C) which was placed close to sample to observe the real time sample temperature as shown in Figure 3.4. Another method of temperature monitor is infrared detector (FLIR) which can be used to detect sample temperature distribution profile to confirm the real temperature of the sample.

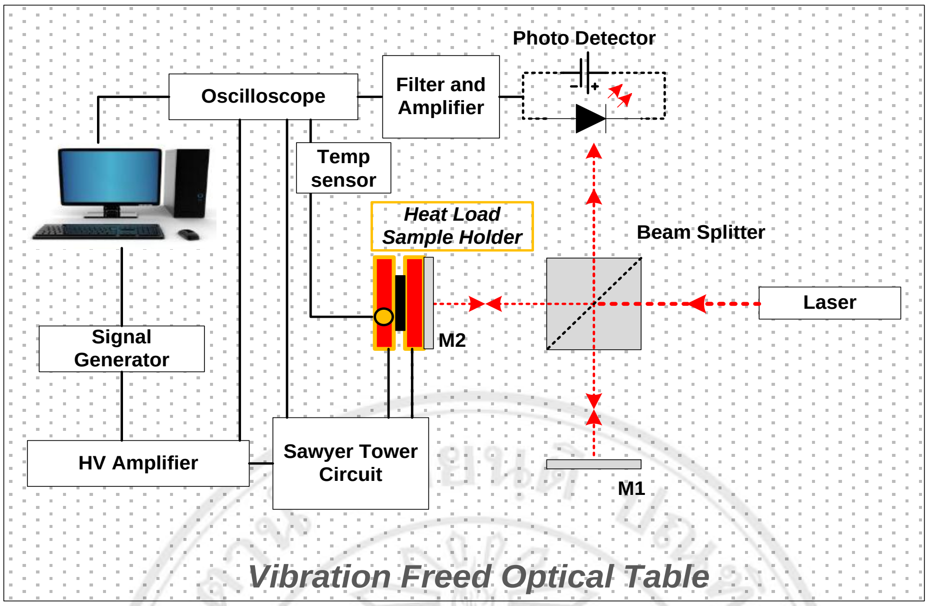

Figure 3.3 Schematic diagram of heat load setup with modified Michelson interferometer for induced-strain measurement system

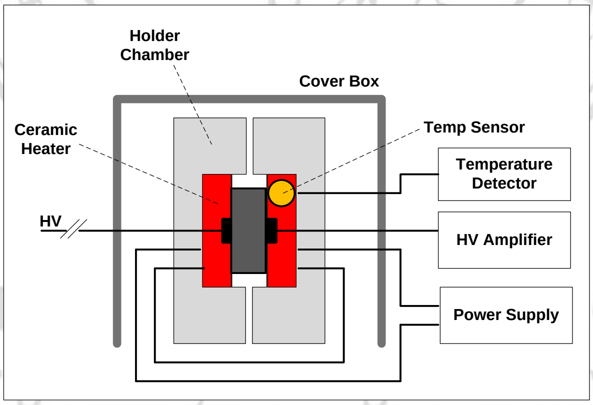

Figure 3.4 The heat load sample holder

To observe temperature dependence, the electric field induced-strain and polarization at various temperature in the range of 30°C to 70°C, was measured using the setup as shown in Figure 3.3. Lead based ferroelectric ceramics ($1-x$)Pb($Mg_{1/3}Nb_{2/3}$)O_3–xPb($Zr_{0.52}Ti_{0.48}$)O_3 ($1-x$)PMN-xPZT ,where x = 0, 0.1, 0.3, 0.5 and

0.7, $(1-x)Pb(Mg_{1/3}Nb_{2/3})O_3-xPbTiO_3$ $(1-x)$PMN-xPT, where x = 0.1, 0.2 and 0.3, and $Pb_{0.91}La_{0.09}(Zr_xTi_{(1-x)})_{0.9775}O_3$ PLZT (9/100x/100-100x), where x = 0.70 and 0.65, were prepared by solid state oxide mixing and consolidating by sintering method. In the measurement, the silver paint was applied at both sides of sample surface and then placed in the heat load sample holder as shown in Figure 3.4. The sample was subjected to a bipolar high extension voltage at 0.2 Hz of frequency from high voltage amplifier/controler supply (Trek 610D). At the time of measurement, the sample temperature was controled at 30, 40, 50, 60 and 70°C according to applied electrical current past through to ceramic heater by the programmable dc power supply (Rigol DP 1116A). The electrical signal from displacement interference intensity was filtered and amplified before detected together with Sawyer-Tower circuit signal and 1/1000 reduce ratio of high voltage signal by 14 bits digital oscilloscope, which had interface to record data at the computer where electric field induced-strain-polarization (s-P-E) and induced-strain as a function of polarization (s-P) were calculated, plotted and ferroelectric behavior as a function of temperature was analyzed.

3.3 Investigation of magnetoelectric properties using modified Michelson interferometer

In order to investigate the effect of magnetic field (B) to induced strain behavior of ferroic materials, the solenoid coil was designed to apply the magnetic field to the sample inside sample holder. The modified Michelson interferometer with solenoid coil was setup at the movable mirror M_1 was shown in Figure 3.5. The magnetic field was changed as a function of the electrical current from the programmable dc power supply (Rigol DP 1116A), and was detected by the gauss meter (ST probe; the magnetic range 0-30 kG) which measured magnetic field along center position of solenoid coil where ferroic sample was placed to observe the actual real magnetic field at sample position as shown in Figure 3.6.

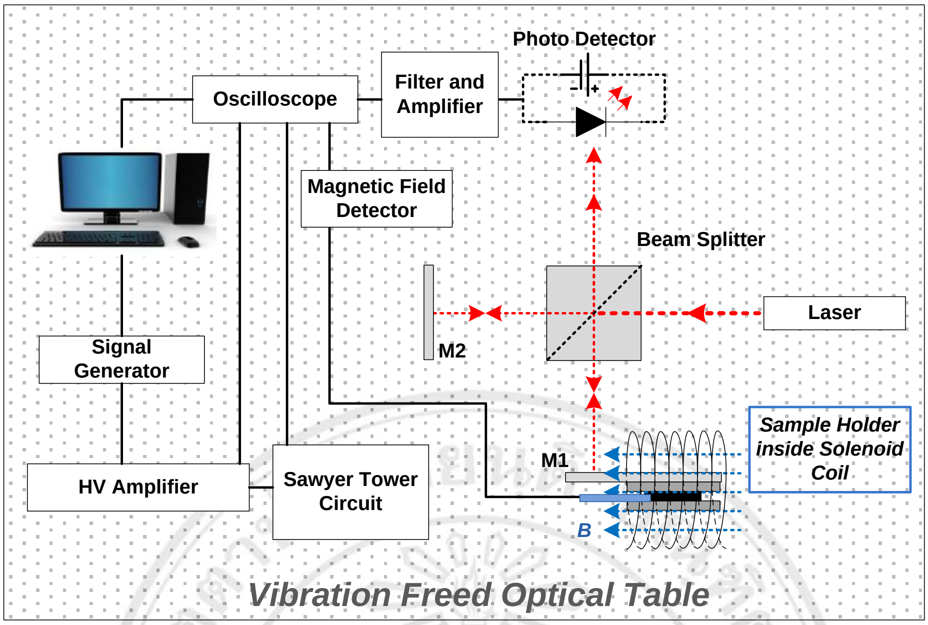

Figure 3.5 Schematic diagram of solenoid coil setup with modified Michelson interferometer for induced-strain measurement system

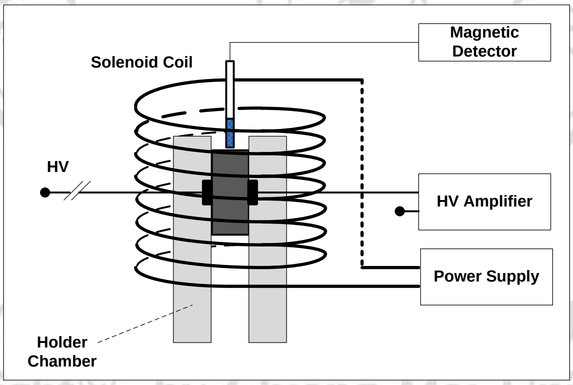

Figure 3.6 The solenoid coil

To observe the effect of magnetic field (B) to induced strain behavior, the electric field induced-strain and polarization at various magnetic field condition was setup as shown in Figure 3.5 to measure magnetoelectric properties of Lead based ferroelectric ceramics, $(1-x)Pb(Mg_{1/3}Nb_{2/3})O_3–xPb(Zr_{0.52}Ti_{0.48})O_3$ $(1-x)$PMN-xPZT ,where x = 0, 0.1, 0.3, 0.5 and 0.7, $(1–x)Pb(Mg_{1/3}Nb_{2/3})O_3–xPbTiO_3$ $(1-x)$PMN-xPT, where x = 0.1, 0.2

and 0.3, and $Pb_{0.91}La_{0.09}(Zr_xTi_{(1-x)})_{0.9775}O_3$ PLZT (9/x/1-x), where x = 0.70 and 0.65 ceramics were prepared by solid state oxide mixing and consolidating by sintering method . In the measurement, the sample was silver glued at the both sides of surface and placed in sample holder inserted inside at the center of solenoid coil for static applied magnetic field condition as shown in Figure 3.6. The sample was subjected to a bipolar high extension voltage at 0.2 Hz of frequency from high voltage amplifier/controller supply (Trek 610D). At the time of measurement, the magnetic field was adjusted according to applied electrical current past through the solenoid coil by the programmable dc power supply (Rigol DP 1116A). The electrical signal from displacement interference intensity was filtered and amplified before detected together with Sawyer-Tower circuit signal and 1/1000 reduce ratio of high voltage signal by 14 bits digital oscilloscope, which had interface to record data at the computer where electric field induced-strain-polarization (s-P-E) and induced-strain as a function of polarization (s-P) were calculated, plotted and ferroelectric behavior as a function of static magnetic field was analyzed.

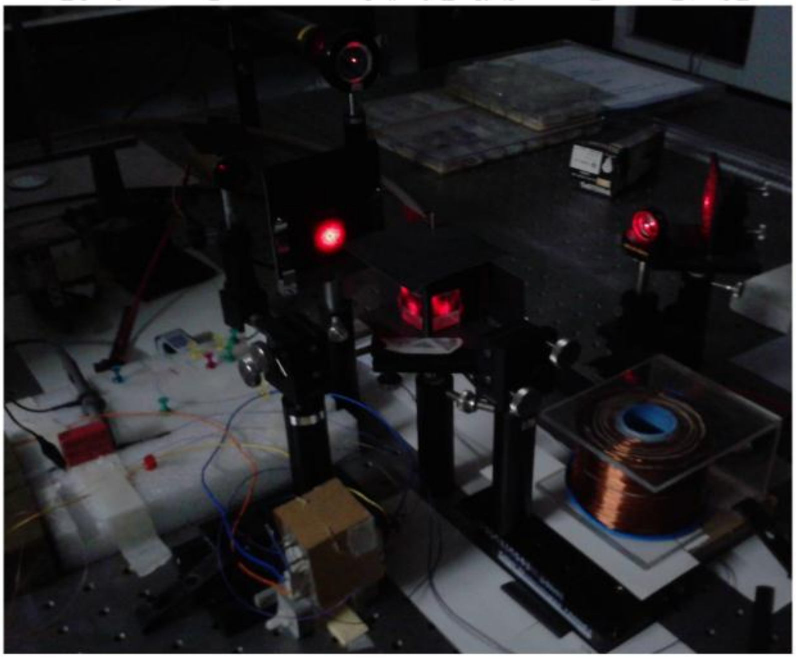

Figure 3.7 Modified Michelson interferometer with heat and magnetic field load for induced-strain measurement system

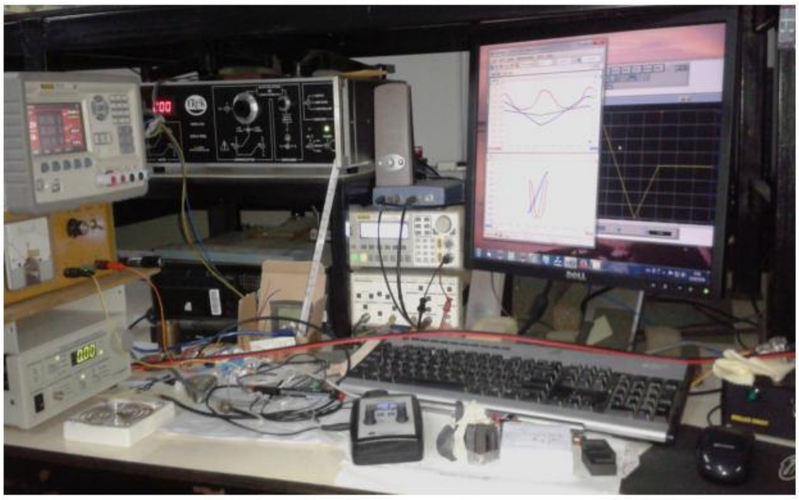

Figure 3.8 The (electronic) instrumental system for induced-strain measurement

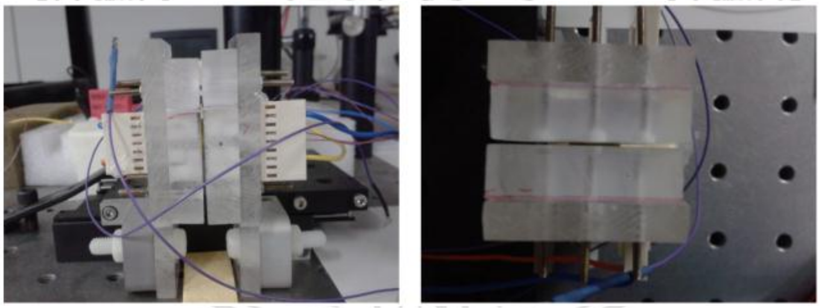

Figure 3.9 The heat load sample holder

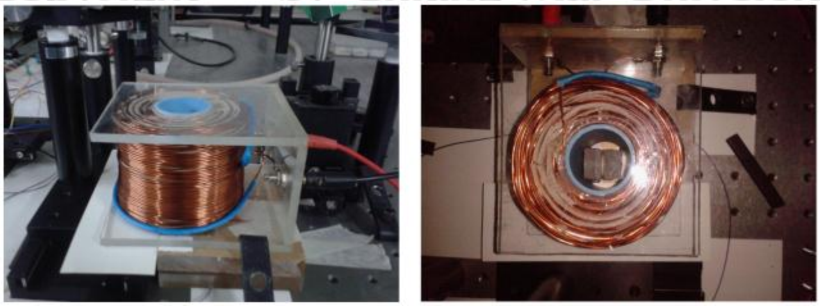

Figure 3.10 The sample holder inside a solenoid coil

3.4 Operating principle

The displacement resulting from electric field induced-strain of ferroic materials was measured by modified Michelson interferometer in terms of interference intensity at the center of circular fringe pattern as shown in Figure 3.11 using photodiode detector (PIN 7787-2). The reverse bias signals from photodiode detector circuit were frequency filtered to eliminate high frequency electrical noises from electrical system, then subjected to signal amplification to gain the signal with suitable amplitude by the low-noise preamplifier (Stanford Research system model SR 560). The amplified signals of displacement interference intensities and the 1/1000 reduced ratio signal of applied high voltage were detected together by the 14 bits digital oscilloscope and recorded at the computer, the detected signal is shown in Figure 3.12.

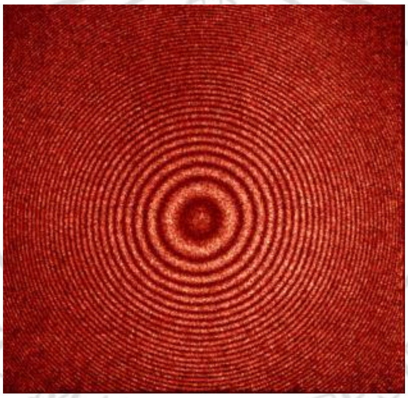

Figure 3.11 The circular fringe pattern when the light passes through Michelson interferometer

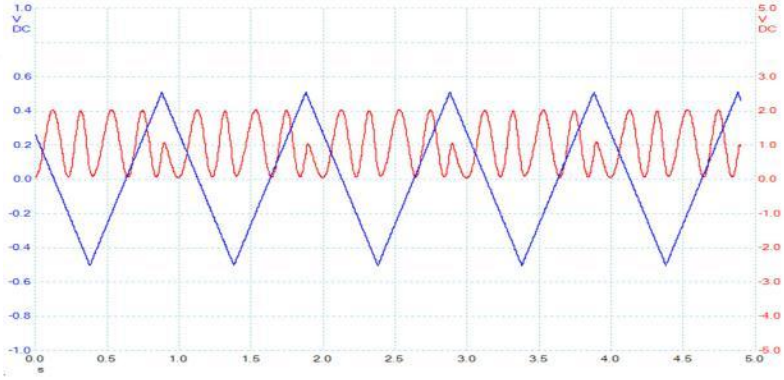

Figure 3.12 The interference intensity (red) and ratio of high voltage (blue)

In Figure 3.12, the maximum to minimum interference intensities (red line) from path difference is equal to the quarter wavelength (λ/4) of the used laser beam source (Helium-Neon laser; MELLES GRIOT, wavelength 632.8nm). The interference intensities (I) related to the displacement (Δd) in equation (2.8) can be written as equation (3.1) [12,37-40].

$$I = I_p + I_r + 2\sqrt{I_p I_r}\cos(\frac{4\pi\Delta d}{\lambda}) \tag{3.1}$$

where I_p is the observing beam intensities and I_r is the reference beam intensities.

Likewise, at the photo diode detector, the interference intensities can be written as

$$I = \frac{1}{2}(I_{\max} + \mathrm{I}_{\min}) + \frac{1}{2}(I_{\max} - \mathrm{I}_{\min})\cos(\frac{4\pi\Delta d}{\lambda}) \tag{3.2}$$

where I_{max} is the maximum interference intensity and I_{min} is the minimum interference intensity of two beams.

All signals are detected by digital oscilloscope (PicoScope) as voltage signals. So, the interference intensities (I) detected as voltage (V) can be written from equation (3.2) as;

$$V = \frac{1}{2}(V_{\max} + V_{\min}) + \frac{1}{2}(V_{\max} - V_{\min})\cos(\frac{4\pi\Delta d}{\lambda}) \tag{3.3}$$

where V_{max} is the maximum voltage detected and V_{min} is the minimum voltage detected from the interference.

The first term of equation (3.3) replies the mean value of detected voltage and the second term replies to the variation of interference voltage (amplitude) of cosine wave function which is proportional to the displacement (Δd) divided by the quarter wavelength ($\lambda/4$). The displacement length can be calculated as equation (3.4).

$$\Delta d = \left(\frac{\lambda}{4\pi}\right)\cos^{-1}\left(\frac{V-\left(\frac{1}{2}(V_{\max}+V_{\min})\right)}{\frac{1}{2}(V_{\max}-V_{\min})}\right) \tag{3.4}$$

Then induced-strain (s) of ferroelectric samples can be calculated as equation (3.5).

$$s = \frac{\Delta d}{d_0}\times 100 \tag{3.5}$$

where d_0 is the thickness of sample.

The induced strain of ferroic material is related to electrical field in two ways. First is piezoelectric effect, where the induced-strain is in linear relationship with applied electrical field. Second is electrostriction, where induced-strain is proportional to square of applied electrical field. Therefore, the relation of induced strain (s_{33}) with applied electric field (E_3) in the same direction (Fig. 3.13) can be written as [1,42];

$$s_{33} = d_{33}E_3 + M_{33}E_3E_3 \tag{3.6}$$

where d_{33} is the piezoelectric tensor components and M_{33} is the electrostriction tensor component in the same direction.

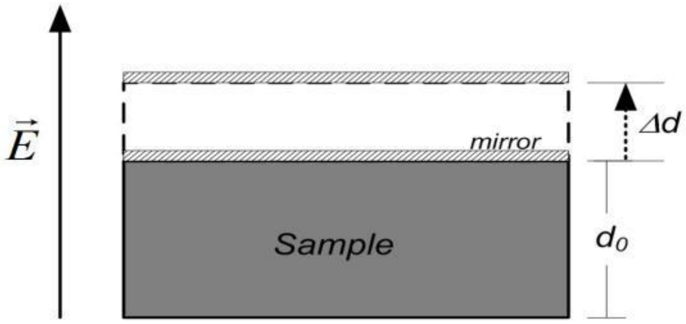

Figure 3.13 Displacement in the direction of applied electric field

Another properties of ferroelectric is electric field induced polarization of ferroic materials and it is measured by Sawyer-Tower circuit as shown in Figure 3.14. The polarization signals from reference capacitor (C_{ref}) is proportional to the polarization of ferroic materials. A 1 μF ceramic capacitor is used as reference capacitor and the voltage across is measured as reference voltage (V_{ref}). The reference voltage and the 1/1000 reduced ratio signal of applied high voltage are detected together by the 14 bits digital oscilloscope and recorded at the computer, the detected signals is shown in Figure 3.15.

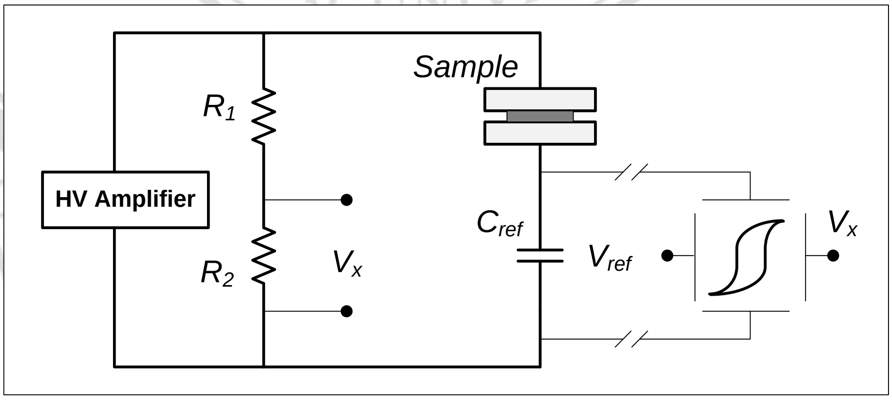

Figure 3.14 Sawyer-Tower circuit

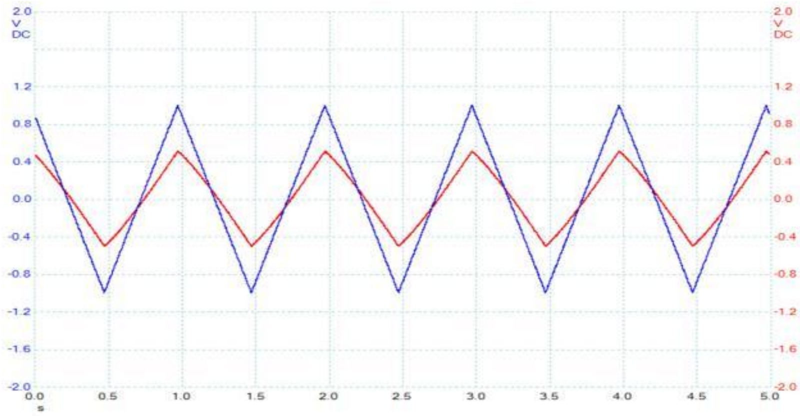

Figure 3.15 The Sawyer-Tower circuit signals (red) and ratio of high voltage (blue)

The polarization **(*P*)** of the ferroelectric sample can be calculated from the across voltage of the reference capacitor, the relation can be written as;

$$P = \frac{C_{ref} V_{ref}}{A} \tag{3.7}$$

where C_{ref} is capacitance of reference capacitor, V_{ref} is voltage across capacitor and A is an area of the sample perpendicular and subjected to electric field.

Therefore, the induced-strain (s) caused by polarization (P) is the quadratic relation and can be written as [1];

$$s = QP^2 \tag{3.8}$$

where P is polarization and Q is the electrostriction tensor component.

The electrical signals from ferroic sample with characteristic of hysteresis of polarization and strain, where the induced-strain signal from displacement interference intensity (red line), the polarization signal from Sawyer-Tower circuit (blue line) and the 1/1000 reduced ratio signal of applied high voltage from high voltage power supply (black line) are measured together as a function of time (s; second) by 14 bits digital oscilloscope in the voltage range -5 to 5 V is shown in Figure 3.16. Then the electrical signals are calculated by equation (3.5) and (3.7) to polarization (blue line) and induced-strain (red line) respectively and then plotted as a function of time (s) as shown in Figure 3.17. The resolution of the induced strain measurement refers to the conversion of an analog to a digital signal in 14-bit digital number.

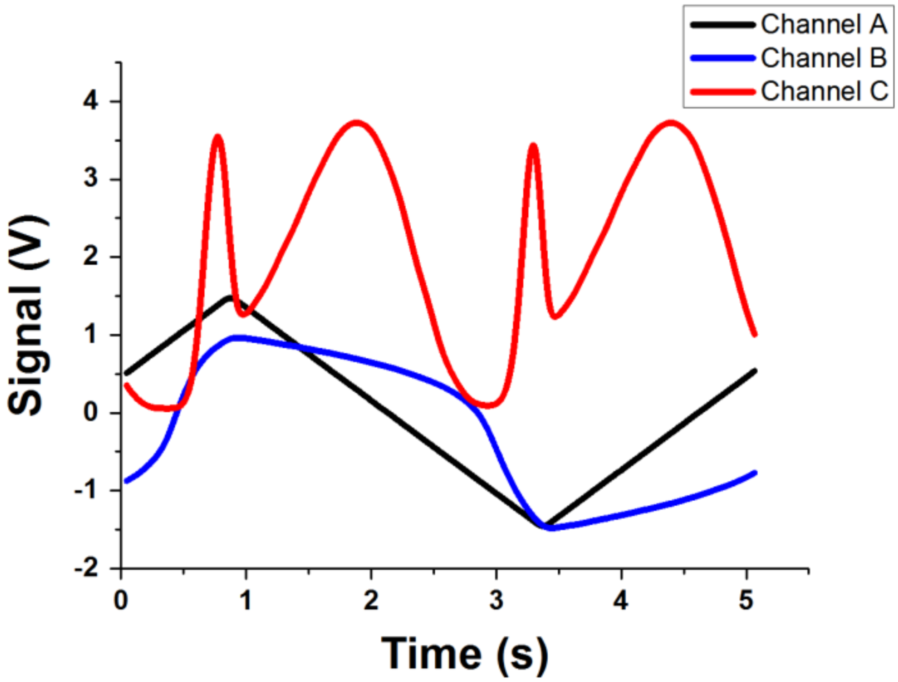

Figure 3.16 The voltage measured signals of ferroic materials

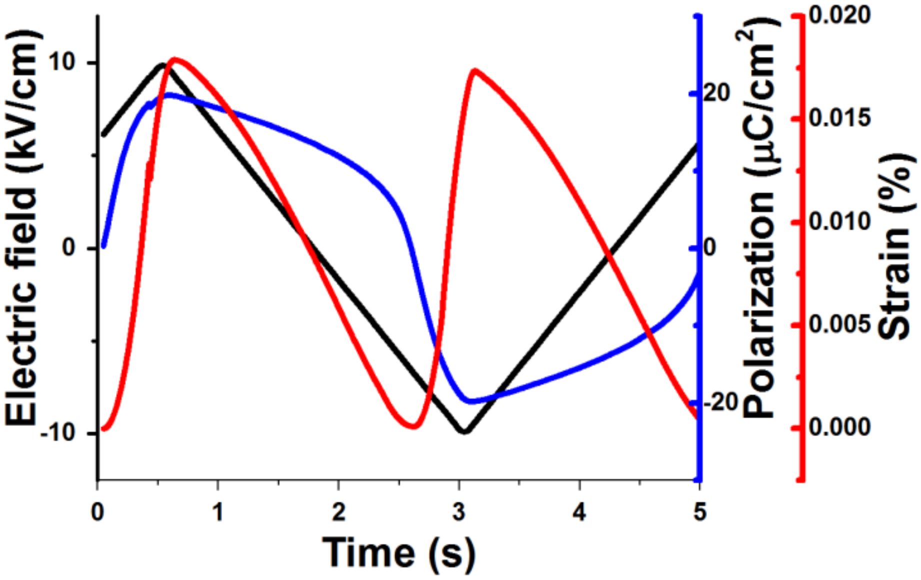

Figure 3.17 The polarization (blue line), induced-strain (red line) and electric field (black line) of ferroic materials

The polarization (blue line) and induced-strain (red line) can be plotted as a function of electric field as shown in Figure 3.18.

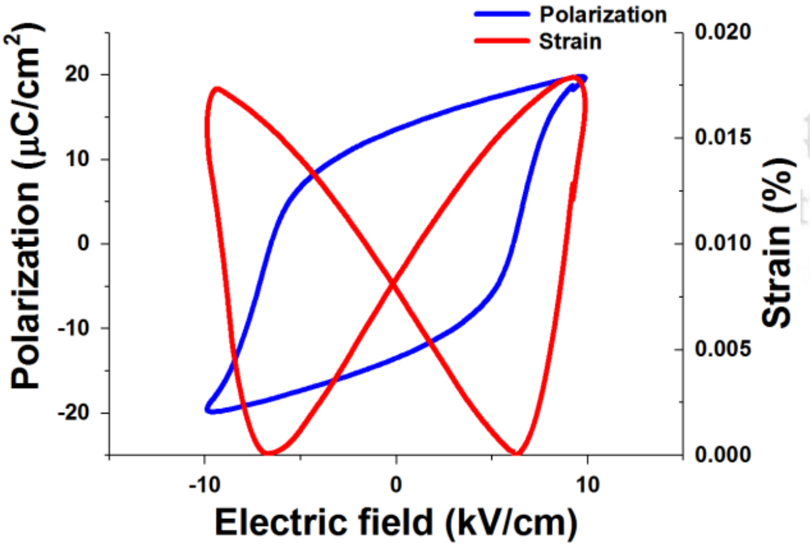

Figure 3.18 The polarization (blue line) and induced-strain (red line) as a function of electric field of ferroic materials

The hysteresis of polarization (U_h; hysteresis loss) is calculated as integrated close loop of *P*-*E* equation referring to the energy loss and the other integrated area is *s*-*E* relation (U_d; piezoelectric loss). The hysteresis loss area of polarization and induced-strain can be written as equation (3.9) and (3.10) respectively;

$$U_h = \int PdE \tag{3.9}$$

$$U_d = \int sdE \tag{3.10}$$

And induced-strain plotted as a function of polarization is shown in Figure 3.19 to obtain *s*-*P* quadratic relation of ferroic materials.

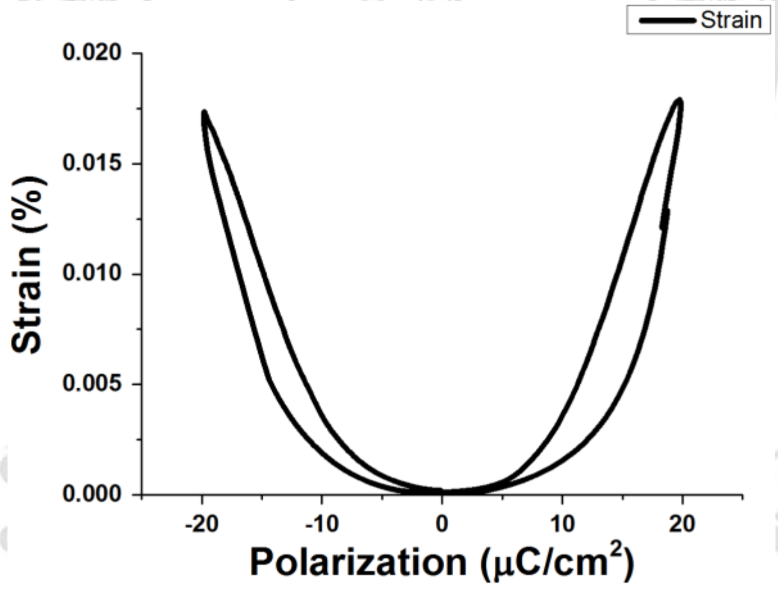

Figure 3.19 The induced-strain plotted as a function of polarization